
Geostatistical Analysis of Spatial Distribution of *Endoclita signifer* Larvae on Eucalyptus

Xiuhao Yang^{1,*}, Jianglin Qin², Youqing Luo³, Zhongwu Yang⁴, Jiguang Wei⁵

¹Department of Guangxi Forestry Pest Management, Bureau of Guangxi Forestry, Nanning, China

²Guangxi Institute of Meteorological Disaster-Reducing Research, Nanning, China

³Forestry College, Beijing Forestry University, Beijing, China

⁴Forestry Pest Management Station of Guiling Districts, Guiling, China

⁵Agriculture College, Guangxi University, Nanning, China

Email address:

xhmail-forestry@163.com (Xiuhao Yang), zhouli5850120@163.com (Jianglin Qin), yqluo@bjfu.edu.cn (Youqing Luo),

hhyyzw@126.com (Zhongwu Yang), jiguangwei@gxu.edu.cn (Jiguang Wei)

*Corresponding author

To cite this article:

Xiuhao Yang, Jianglin Qin, Youqing Luo, Zhongwu Yang, Jiguang Wei. Geostatistical Analysis of Spatial Distribution of *Endoclita signifer* Larvae on Eucalyptus. *American Journal of Agriculture and Forestry*. Vol. 6, No. 6, 2018, pp. 226-236. doi: 10.11648/j.ajaf.20180606.20

Received: October 14, 2018; **Accepted:** November 14, 2018; **Published:** December 24, 2018

Abstract: *Endoclita signifer* is a native wood borer species adapted to infest Eucalyptus in Guangxi of China. To better understand its spatial distribution in Eucalyptus forests, geostatistical approach was employed to analyze survey data of small scale (plantation level) and large scale (provincial level). The small scale results showed that the spatial distribution pattern was clumped regardless of infestation level. But the distance of spatial dependence was different with different infestation levels. These distances were 20.0 m, 40.3 m and 69.4 m for light, moderate and severe infestation levels, respectively. This indicated that as infestation level increased, the spatial distribution was less clumped. At the large scale level, the spatial distribution pattern was random when infestation was light. At the moderate and severe infestation level, the distribution pattern was clumped. The distance of spatial dependence was 43.6 km, 15.5 km and 12.47 km for light, moderate and severe infestation, respectively. This trend was opposite to that of the small scale. The large scale survey results reflected the occurrence of *E. signifer* in Guangxi province. Eucalyptus trees are cultivated in every county of Guangxi. Plantations with light infestation were scattered in a random pattern across the province. Moderate and severe infested plantations were mainly distributed in the central and southern areas of the province where Eucalyptus cultivation has longer history compared to other areas. Furthermore, the distance of spatial dependence was 17.4 km and 21.3 km for the 2nd generation forests (ratoon) and the 1st generation forests (established via seedlings), respectively. The observed spatial distribution patterns of *E. signifer* larvae seemed closely related to its biology and its successful adaptation to attack exotic Eucalyptus. These results provide fundamental knowledge for forecasting and evaluating *E. signifer* infestation and damage of Eucalyptus forests.

Keywords: *Endoclita signifer*, Spatial Distribution Pattern, Geostatistics, Eucalyptus

1. Introduction

Endoclita signifer Walker (Lepidoptera: Hepialidae) is a polyphagous wood borer with the host range of 31 woody species in 24 genus and 16 families [1, 2]. The insect is a relatively new pest of Eucalyptus in Guangxi and Guangdong provinces of China [1]. The larvae bore into woody tree trunks or branches, adversely affecting tree growth and causing branch breakage. Young trees can be killed due to

complete girdling causing significant damages to newly established forests. Eucalyptus grows fast. The trees are widely cultivated in southern China for the paper industry, which provides great benefits to local economy [3]. The damage of *E. signifer* to Eucalyptus became more noticeable in recent years due to the vast expansion of Eucalyptus cultivation in the region. A survey in 2012 showed that *E.*

signifer infestations were found in ~3536.3 hm² of Eucalyptus forests distributed in 278 towns of 60 counties in Guangxi [2]. Risk analysis studies indicate that this pest has moderate to high outbreak risk with the risk index of $R=1.911$ ($R>2.5$ as extreme high risk, $2.5>R>2.0$ as high risk, $2.0>R>1.5$ as moderate risk, $1.5>R>1.0$ as low risk, and $R<1.0$ as no risk) [4, 5]. As cultivation of Eucalyptus continues to intensify, the importance of *E. signifer* management increases, which demands better understanding of this insect.

Spatial distribution is an important ecological character of insects with significant implication in pest population forecast and management. For example, spatial distribution can aid the understanding of population dispersal and dynamics; can dictate sampling schemes, e.g. number of samples needed and sample unit size; and can potentially improve control efficiency. Traditionally, spatial distribution patterns are described using parametric statistical methodologies such as negative binomial distribution, Taylor's power law analysis, Iwao's mean crowding regression, index of dispersion, and index of clumping based on sample means and variances [6, 7]. Geostatistics is an applied statistical tool of modeling spatial distribution patterns that allows correlation between sample data and sample location in space. Unlike classical statistics that requires data to be randomly taken and independent, geostatistics can be more appropriate for autocorrelated and non-random sampling data [8, 9]. Geostatistical methods have been used for insect spatial distribution analysis [9, 10]. It can describe the random nature of insect distribution and population structure change more accurately. After model fitting, values at unsampled locations in space can be predicted using algorithms such as ordinary Krigging interpolation.

Although the topic of geostatistical description of insect spatial distribution has been studied [9-14], comparative studies of spatial distribution at different spatial scales are rare. Such studies are important for forestry pests due to more complicated environment. *E. signifer* is a relatively new pest of Eucalyptus forests. Fewer studies have been done about this species. Understanding the spatial distribution of *E. signifer* is fundamentally important. Here we report the geostatistical analysis of spatial distribution patterns of *E. signifer* in Eucalyptus forests at small (individual plantation) and large (province-wide) scales based on survey data collected in 2011-2012. The results can be utilized in developing population monitoring, forecasting and

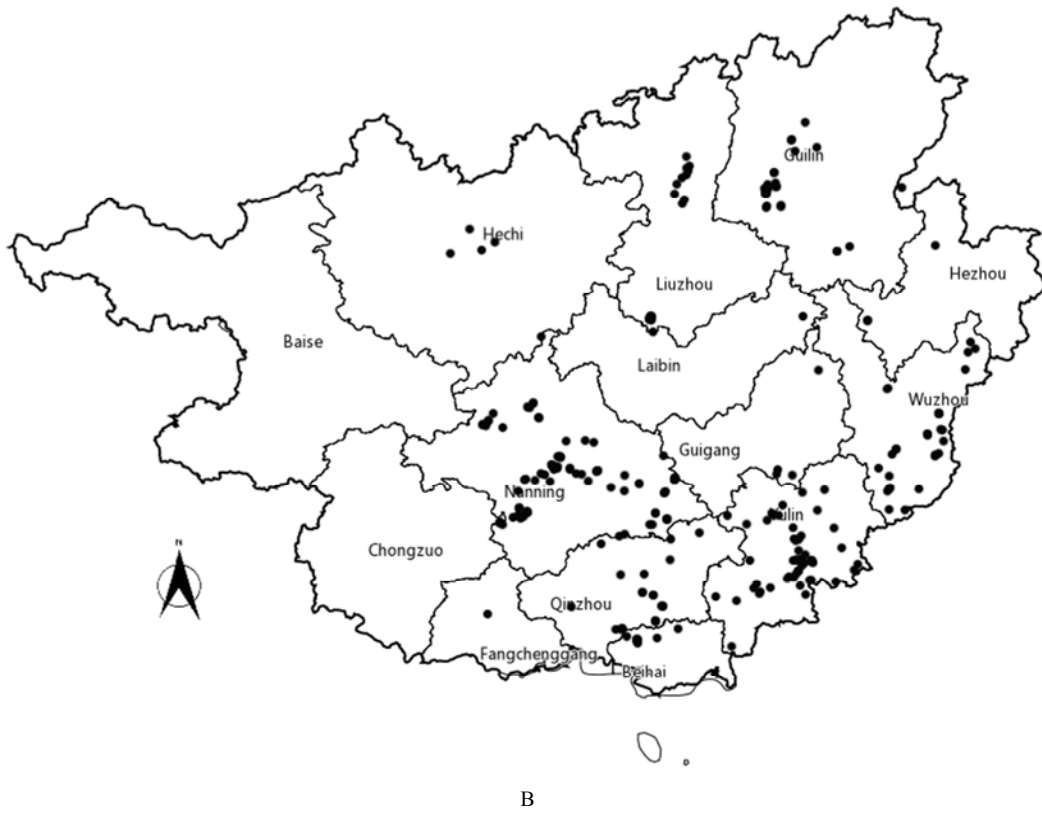
management strategies.

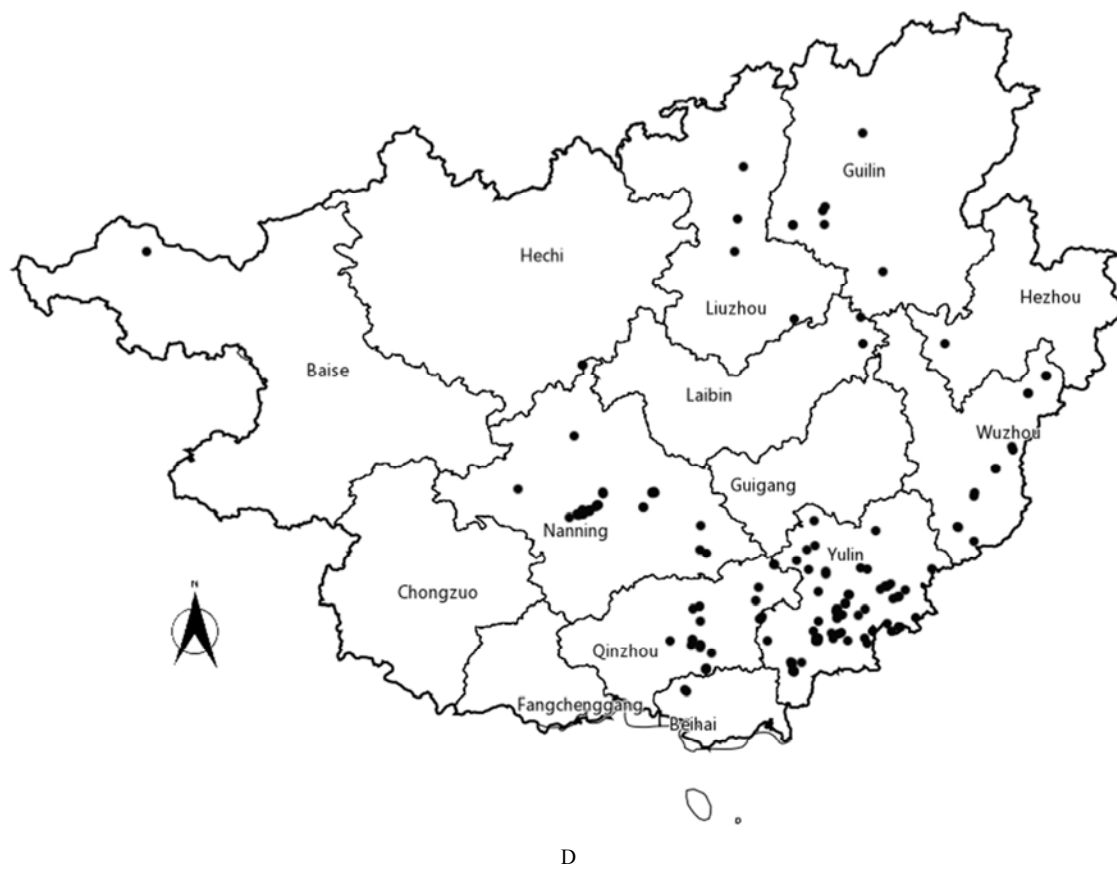
2. Materials and Methods

2.1. Study Areas and Data Collection

Individual plantation (small-scale) surveys were conducted in Nanning, Yuling, and Qinzhou districts, including Wuming, Binyang, Hengxian, Luchuan, Bobai, Beiliu, Lingshang and Pubei counties, and two forestry farms of Gaofeng and Bobai of Guangxi province (Figure1A). The sample area is low hills with high temperature and rainfall that is ideal for Eucalyptus [5, 15]. These counties and forestry farms also are the earliest adaptors to cultivate the fast growing and high yield hybrid Eucalyptus in large acreages. Thus, *E. signifer* infestation is wide spread in the areas with heavy damage, suitable for pest monitoring and management studies. In 2011-2012, detailed records of *E. signifer* were collected in the months of September and October when the presence of *E. signifer* is most apparent with easily recognizable semispherical balls of fresh wood fragments fastened at the point of entry. These visible semispherical balls were counted as number of larvae as *E. signifer* are cryptic borers living inside of tree trunks individually [1]. If a plantation in the designated areas was found to be infested with *E. signifer*, it was set as a sample site. Detailed investigation was conducted by examining 100 trees in a 10 trees \times 10 rows area to record number of larvae per tree. For irregular shaped sample sites, more rows were surveyed until the number of sampled tree reached to 100. The location of each sampled tree was mapped using the 2 \times 3 m tree row spacing on a gridded paper to be used for geostatistical analysis.

The large-scale (provincial level) surveys were conducted in the similar way as the small-scale survey at each sampled plantation (Figure1B-F). All Eucalyptus plantations in the major Eucalyptus cultivation areas of Guangxi were surveyed in July-December of 2011 and 2012. In addition to the number of *E. signifer* larvae per tree, tree species and age, forest type (1st generation=established by tree seedlings; 2nd generation=reestablished forest via ratoon), and sample site's GPS position were recorded as well. The average number of larvae per tree of each site (100 trees were surveyed) and the site GPS coordinates converted to kilometer grid were used for geostatistical analysis.





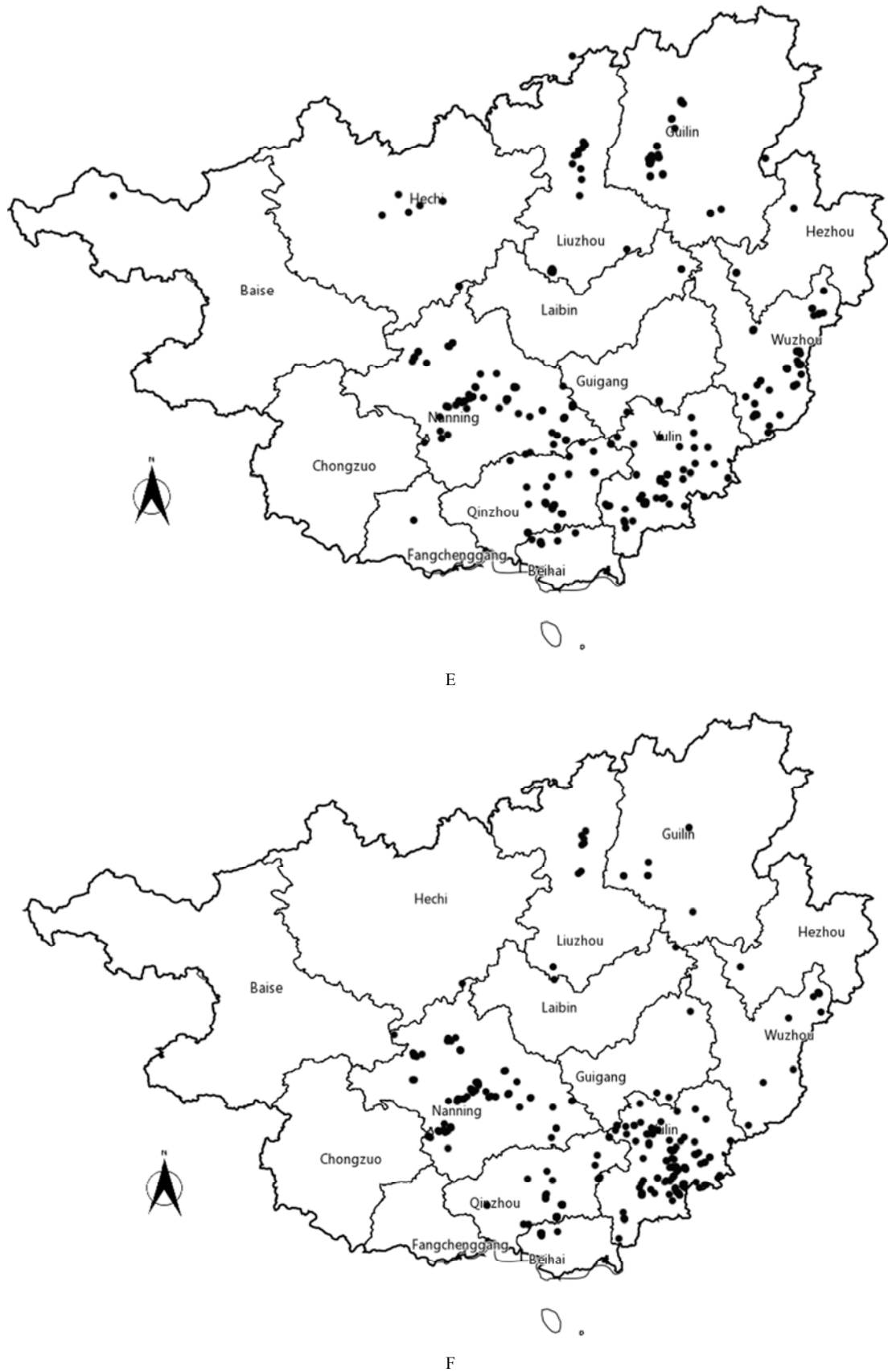


Figure 1. Sample site locations (represented by ●) for the spatial distribution study of *E. signifer* larvae in Guangxi province. A. Sample sites in the small scale survey; B. Light infestation sample sites for the large scale survey; C. Moderate infestation sample sites for the large scale survey; D. Severe infestation sample sites for the large scale survey; E. 1st Generation sample sites; and F. 2nd Generation sample sites.

Each sample site was categorized into three infestation/damage levels according to the percent of infested trees as: light = less than 5%, moderate = 5-10%, and severe = greater than 10% for analysis purpose.

2.2. Geostatistical Analysis

GS+9.0 software (Gamma design Software, Plainwell, Michigan USA) was used [16].

First, to describe the spatial correlations of the empirical data set, semi-variograms were constructed by variogram function [12]:

$$\gamma(h) = \frac{1}{2N(h)} \sum_{i=1}^{N(h)} [Z(x_i) - Z(x_i + h)]^2 \quad (1)$$

Where $\gamma(h)$ is the semi-variance for distance h , $N(h)$ is the number of data pairs separated by h , $Z(x_i)$ is the observed value at location x_i , $z(x_i+h)$ is the value at location x_i+h . Thus, $\gamma(h)$ is the variance of all sample pairs separated by distance h in a given data set. The function is applied to a set of predetermined h and plotted against h . More rapid increase of semi-variogram represents faster deterioration of the influence of a given sample. For the current study, omnidirectional variogram (without considering direction of two sample points) was constructed assuming direction had no effect on *E. signifer* distribution behavior.

Second, the empirical variogram was fitted to theoretical

models including spherical, exponential, Gaussian and linear models. Figure 2 is a generic plot of variogram spherical model illustrating the nugget, sill, and range. Nugget effect (C_0) is the nonzero intercept point at Y axis representing the sampling error and spatial variation due to sampling distance. Sill (C_0+C) is the Y-axis value where the curve stabilizes. The corresponding distance of the sill is the range (α), representing the average distance from a point where some level of spatial correlation exists. Sample locations apart greater than the range are not autocorrelated. The $C/Sill$ ratio represents the degree of sample autocorrelation (spatial dependency). Lower ratio indicates lower correlation, and higher ratio indicates higher correlation. Best model selection mainly depends on correlation coefficient R^2 (higher R^2 indicates better fit), followed by residual sum of square (RSS) (smaller RSS indicates better fit). The range and nugget effect values can also be considered when determine the best fitted model [8, 12, 17-20]. Distribution pattern is reflected by the shape of semivariograms (the best fitted model). Spherical, exponential and Gaussian models suggest clumped distribution. Spatial dependence is gradually reduced as distance increases until the sill in a spherical spatial structure (Figure 2). Exponential structure has nice spatial continuity in short distances, but the continuity drops rapidly at longer distance. Linear model suggests random or uniform distribution with low correlation coefficient and high variation for the random structure [12, 21].

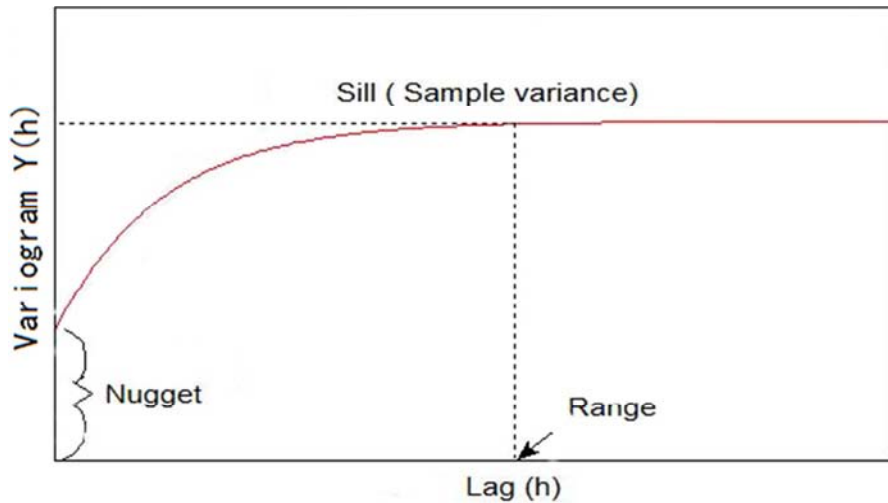


Figure 2. A typical variogram of spherical model illustrating nugget, sill and range.

3. Results

3.1. Geostatistical Description at the Small-Scale Level

A total of 4400 trees in 44 sites (plantations) were surveyed. Among the sample sites, there were 11 sites with light (percent tree infested <5%) or moderate (percent tree infested 5-10%) infestation level each, and 22 sites with severe infestation level (percent tree infested >10%). The mean percent tree infested and the mean number of larvae per

tree was 3.61% and 0.04, respectively, for the light infestation plantations. For moderate and severe infestation plantations, the mean percent tree infested and the mean number of larvae per tree was 7.18% and 0.08, and 23.45% and 0.37, respectively. Geostatistical analysis was performed with the number of larvae using tree as sampling unit. Table 1 shows the model fitting parameters of each infestation category. When infestation was light, none of the models fitted well as all of them with low R^2 . Relatively, spherical model had the best fit with R^2 of 0.206, greater than that of

other models. The RSS was at similar level for all the models. The poor fit could be due to low number of infested trees (high number of zeros in the dataset). The range of the spherical model was 20.0 m (about 10 trees distance) at the low infestation level. The model fitting was much better for plantations with higher infestation levels. The exponential model was the best fit with high R^2 of 0.906 for plantations of moderate infestation level. The range was 40.4 m (about

20 trees distance). The exponential model also was the best fitted model with high R^2 of 0.902 when infestation level was severe. The range was 69.4 m (about 30-35 trees distance). The range increased as the infestation level increased, suggesting that *E. signifer* larval distribution had a certain level of spatial continuity. The distribution of *E. signifer* larvae was classified as clumped based on the type of the best fitted model regardless of infestation level.

Table 1. Geostatistical parameters and spatial distribution of *E. signifer* larvae at small scale plantation level*.

| Damage | Model | Nugget C_0 | C | Range (m) | Sill | $C/Sill$ | R^2 | RSS | Distribution Pattern |
|--------------------------------|-------------|--------------|----------|-----------|----------|----------|-------|------------------------|----------------------|
| Light 0.04** 3.91%*** | Linear | 0.000738 | 0.0047 | 18.7232 | 0.005438 | 0.128 | 0.100 | 1.354×10^{-6} | Clumped |
| | Spherical | 0.00001 | 0.00512 | 20.000 | 0.005130 | 0.998 | 0.205 | 1.703×10^{-6} | Clumped |
| | Exponential | 0.00001 | 0.00512 | 0.1500 | 0.005130 | 0.998 | 0.000 | 1.703×10^{-6} | Clumped |
| Moderate 0.08** 7.18%*** | Gaussian | 0.00001 | 0.00512 | 0.5543 | 0.005130 | 0.981 | 0.000 | 1.703×10^{-6} | Clumped |
| | Linear | 0.007202 | 0.005871 | 18.7232 | 0.013073 | 0.449 | 0.932 | 1.810×10^{-6} | Clumped |
| | Spherical | 0.00001 | 0.01091 | 3.9900 | 0.010920 | 0.999 | 0.378 | 2.523×10^{-6} | Clumped |
| Severe 0.37** 23.45%*** | Exponential | 0.006750 | 0.01075 | 40.380 | 0.01750 | 0.614 | 0.906 | 2.523×10^{-6} | Clumped |
| | Gaussian | 0.00001 | 0.01091 | 3.2216 | 0.01092 | 0.999 | 0.380 | 1.648×10^{-5} | Clumped |
| | Linear | 0.023077 | 0.02733 | 18.7232 | 0.05041 | 0.542 | 0.897 | 6.178×10^{-5} | Clumped |
| | Spherical | 0.02180 | 0.0315 | 27.290 | 0.05330 | 0.591 | 0.896 | 6.212×10^{-5} | Clumped |
| | Exponential | 0.01790 | 0.0405 | 69.420 | 0.05840 | 0.693 | 0.902 | 5.848×10^{-5} | Clumped |
| | Gaussian | 0.0260 | 0.0261 | 22.101 | 0.05210 | 0.501 | 0.856 | 8.650×10^{-5} | Clumped |

*Best fitted model is in Bold
 ** Mean number of larvae per tree
 ***Mean percent infested trees

In this current analysis, $C/Sill$ ratio was higher at light infestation (0.998) than that at moderate and severe infestation (0.614, 0.693, respectively). This suggests that at plantation level, the *E. signifer* larval spatial distribution was less spatially depended as the infestation levels increased, where the distribution tended to be more random. Figure 3 (A, B and C) shows the variograms of the light, moderate and severe infestation levels. These plots demonstrate that the spatial correlation explained 99.8%, 61.4% and 69.3% of spatial variability in plantations with light, moderate and severe infestation levels, respectively. As infestation level increased, *E. signifer* larvae were less spatially depended and more randomly distributed.

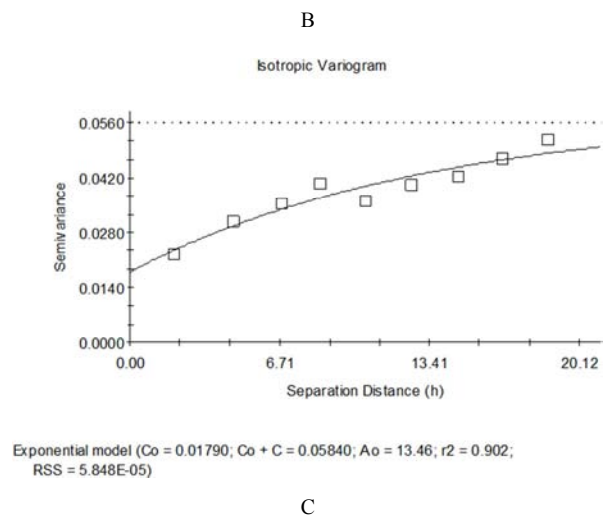
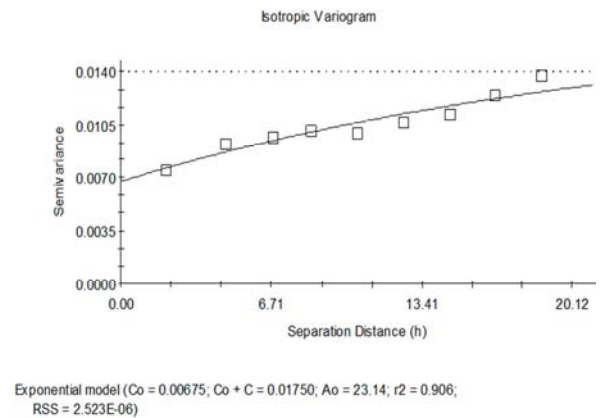
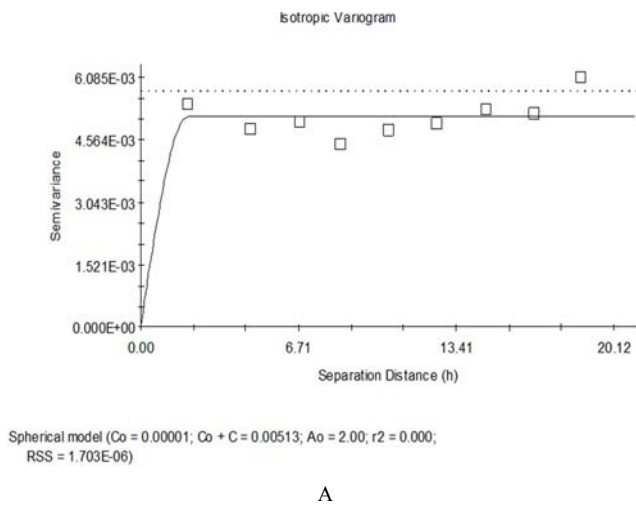


Figure 3. Spatial variograms of *E. signifer* larvae in light (A), moderate (B), and severe (C) infested/damaged *Eucalyptus* plantations of the small scale survey.

3.2. Geostatistical Description at Large-Scale Level

The large-scale level survey included 811 plantations across the entire Guangxi province. Among them, 445, 164 and 202 plantations were categorized as light, moderate and severe infestation level, respectively. In regard of forest type, 448 plantations were the 1st generation forest and 363 were the 2nd generation forest. The mean percent tree infested and the mean number of larvae per tree was 2.78% and 0.03, respectively, for the light infested plantations. For moderate infested plantations, they were 7.48% and 0.01 larvae per tree, respectively. For the severe infested plantations, they were 25.52% and 0.49 larvae per tree, respectively. The mean percent tree infested and the mean number of larvae per tree was 6.38% and 0.08, respectively for the 1st generation plantations; and 10.66% and 0.18, respectively for the 2nd generation plantations.

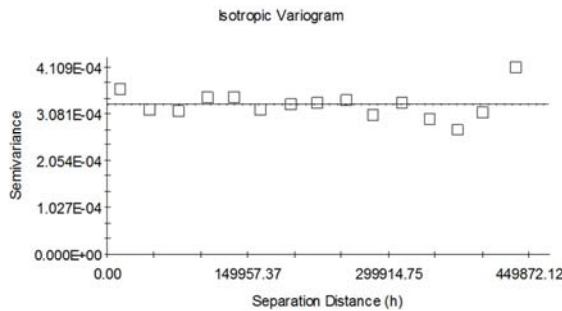
Geostatistical analysis was performed with the average number of larvae per tree using plantations as sample units. At the large-scale level, linear without sill model was the best fitted model when infestation level is light, while spherical

model and Gaussian model were the best fit models when infestation level was moderate and severe, respectively (Table 2). This *E. signifer* distribution pattern would be related to uneven distribution of Eucalyptus in Guangxi. The spatial distribution of *E. signifer* larvae at light infestation level was random, while at moderate and severe infestation levels the distribution was clumped based on the type of the best fitted model. The variograms of the best fitted models showed that the C/sill ratio increased as the infestation intensified (0, 0.666 and 0.899 for light, moderate and severe infestation levels, respectively). The range decreased as the infestation increased (43.6 km, 15.5 km, and 12.5 km for light, moderate and severe infestation levels, respectively) (Figure 4A-C). These results suggest that the distribution of *E. signifer* larvae had a level of spatial continuity. This continuity became weaker as the distance increased. The spatial correlation explained 0%, 66.6% and 89.9% of spatial variability at light, moderate and severe infestation levels, respectively, suggesting that spatial correlation increased as infestation increased. This trend is opposite to the small-scale level.

Table 2. Geostatistical parameters and spatial distribution of *E. signifer* larvae at large scale level*.

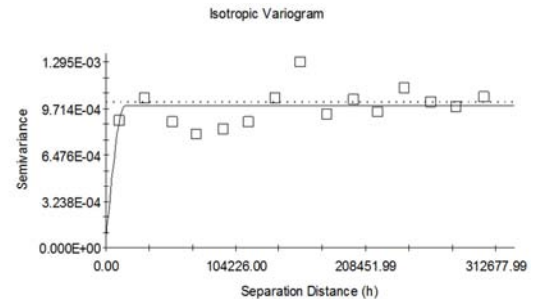
| Damage | Model | Nugget C_0 | C | Rangea | Sill | C/Sill | R^2 | RSS | Distribution pattern |
|---|-------------|--------------|---------|--------|--------|--------|--------|------------------------|----------------------|
| Light 0.03** 2.78%*** | Linear | 0.0003 | 0.0000 | 43602 | 0.0003 | 0.0000 | 0.1860 | 1.369×10^{-7} | Random |
| | Spherical | 0.0002 | 0.0001 | 14600 | 0.0003 | 0.9360 | 0.0025 | 1.370×10^{-7} | Clumped |
| | Exponential | 0.0004 | 0.0000 | 900 | 0.0004 | 0.8840 | 0.0000 | 1.369×10^{-7} | Clumped |
| Moderate 0.10** 7.48%*** | Gaussian | 0.0005 | -0.0002 | 3989 | 0.0003 | 0.8210 | 0.0000 | 1.370×10^{-7} | Clumped |
| | Linear | 0.0009 | 0.0002 | 302888 | 0.0011 | 0.1620 | 0.1790 | 1.829×10^{-7} | Clumped |
| | Spherical | 0.0000 | 0.0009 | 15500 | 0.0009 | 0.6660 | 0.4320 | 2.135×10^{-7} | Clumped |
| Severe 0.49** 25.52%*** | Exponential | 0.0001 | 0.0008 | 15600 | 0.0009 | 0.8810 | 0.0420 | 2.138×10^{-7} | Clumped |
| | Gaussian | 0.0001 | 0.0008 | 13337 | 0.0009 | 0.8710 | 0.0430 | 2.136×10^{-7} | Clumped |
| | Linear | 0.2925 | 0.1463 | 303894 | 0.4388 | 0.3330 | 0.1310 | 0.1890 | Clumped |
| 1 st Generation 0.08** 6.38%*** | Spherical | 0.0460 | 0.3250 | 14600 | 0.3710 | 0.8760 | 0.0080 | 0.2160 | Clumped |
| | Exponential | 0.0530 | 0.3180 | 15000 | 0.3710 | 0.8570 | 0.0108 | 0.2160 | Clumped |
| | Gaussian | 0.0746 | 0.2966 | 12470 | 0.3712 | 0.8990 | 0.5801 | 0.2160 | Clumped |
| 2 nd Generation 0.18** 10.66%*** | Linear | 0.1135 | 0.0000 | 437469 | 0.1135 | 0.0000 | 0.0262 | 0.0230 | Clumped |
| | Spherical | 0.0143 | 0.0993 | 14700 | 0.1136 | 0.8740 | 0.1320 | 0.2330 | Clumped |
| | Exponential | 0.0010 | 1.4660 | 21300 | 1.4670 | 0.6999 | 0.5810 | 0.3320 | Clumped |
| | Gaussian | 0.0310 | 0.0820 | 4157 | 0.1130 | 0.7260 | 0.0063 | 0.2330 | Clumped |
| | Linear | 0.1052 | 0.1922 | 312880 | 0.2974 | 0.6460 | 0.0670 | 0.0557 | Clumped |
| | Spherical | 0.0164 | 0.2116 | 76300 | 0.2280 | 0.9260 | 0.2870 | 0.7450 | Clumped |
| | Exponential | 0.0930 | 0.3180 | 17420 | 0.4110 | 0.9787 | 0.4600 | 0.5650 | Clumped |
| | Gaussian | 0.0347 | 0.1867 | 56291 | 0.2214 | 0.8430 | 0.2980 | 0.0744 | Clumped |

*Best fitted model is in Bold
 ** Mean number of larvae per tree
 ***Mean percent infested trees



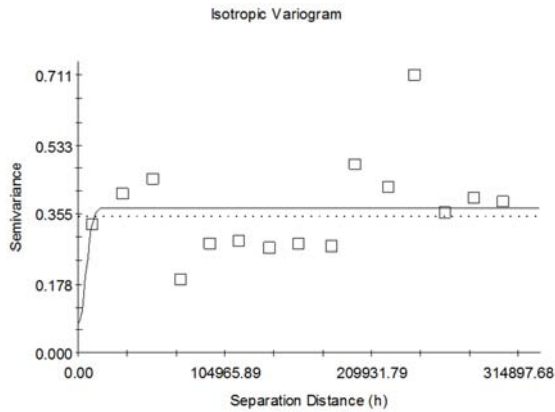
Linear model ($C_0 = 0.00033$; $C_0 + C = 0.00033$; $A_0 = 436085.28$; $r^2 = 0.005$; $RSS = 1.369E-08$)

A



Spherical model ($C_0 = 0.00003$; $C_0 + C = 0.00100$; $A_0 = 15500.00$; $r^2 = 0.043$; $RSS = 2.135E-07$)

B



Gaussian model ($C_0 = 0.07460$; $C_0 + C = 0.37120$; $A_0 = 7200.00$; $r_2 = 0.008$; $RSS = 0.216$)

C

Figure 4. Spatial variograms of *E. signifier* larvae in light (A), moderate (B), and severe (C) infested/damaged *Eucalyptus* plantations of the large scale survey.

The exponential model was the best fitted model for both 1st and 2nd generation forests. The variogram plots (Figure 5A and 5C) and the interpolation forecast maps (Figure 5B and

5D) show that the distribution of *E. signifier* larvae was clumped for both types of forests. However, *C/Sill* ratio of the 2nd generation forests (0.9787) was higher than that of the 1st generation forests (0.6999). The range (α) of the 2nd generation forests (17.4 km) was smaller than that of the 1st generation forests (21.3 km). These results suggest that the distribution of *E. signifier* larvae in the 2nd generation forests was more clumped and spatially depended than that in the 1st generation forests. The spatial correlation explained 97.8% and 69.6% of spatial variability of the 2nd and the 1st generation forests, respectively. The interpolation map of the 1st generation forests (Figure 5B) reflected *E. signifier* larvae distributed across the whole region where the east and southwest areas were heavier. In the 2nd generation forests (Figure 5D), *E. signifier* larvae were distributed mainly in the east, central, and southeast areas, where the southeast area was heavier. These interpolated results corresponded with the *E. signifier* survey results of 2012 (Yang et al. 2013b) and *Eucalyptus* cultivation practice in Guangxi. *Eucalyptus* plantations mainly distributed in the east, central and southeast areas of Guangxi before 2005. These older plantations were 2nd generation forests with heavier *E. signifier* infestation and damage.

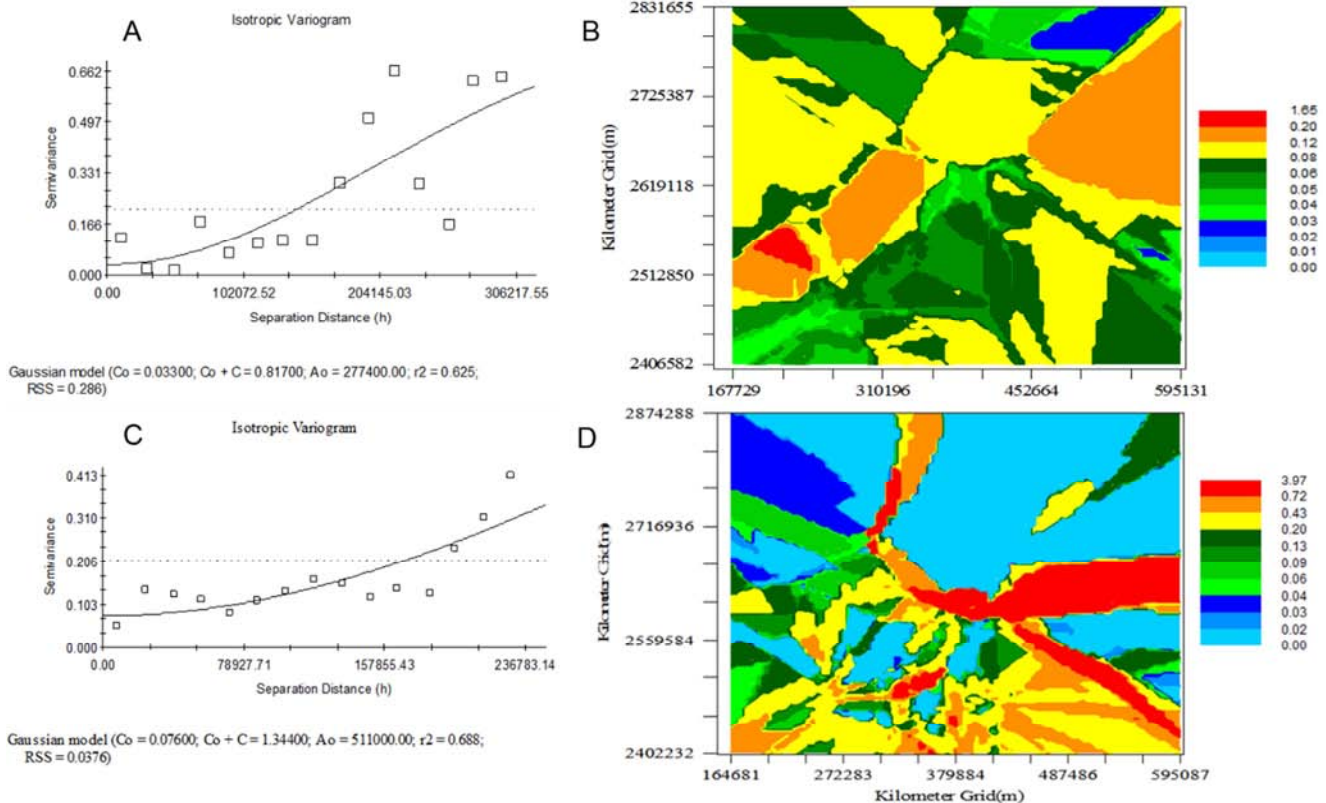


Figure 5. Spatial variograms and interpolation forecast diagram of the population of *E. signifier* larvae in *Eucalyptus* plantations. (A) Spatial variogram in the new planted plantations (1st generation forests); (B) Interpolation of population forecast map of the newly planted plantations; (C) Spatial variogram in the ratoon plantations (2nd generation forests); (D) Interpolation of population forecast map of the ratoon plantations.

4. Discussion

Spatial distribution pattern is very much depended on insect biology, behavior, population density and

environment. The results of geostatistical analysis of this study were similar to that of traditional statistical approaches [22]. The geostatistical analysis at the small scale level (plantation) suggested that *E. signifier* larval distribution was

clumped regardless of infestation levels. However, the spatial dependency and range were different depending on the infestation level. As the infestation level increased, *E. signifer* larval distribution was less spatially correlated. Plantations of light infestation level often are experiencing initial invasion of *E. signifer* larvae from wild hosts. As the result, the infestation normally is isolated at 1 or 2 tree-row on the edge close to wild hosts (sources), *E. signifer* distribution is more clumped. As the infestation progresses, *E. signifer* larvae are more randomly distributed across the whole plantation. This would be due to resource competition and that *E. signifer* larvae are territorial or mutually exclusive [12, 23, 24]. This finding is similar to the spatial distribution trend of gypsy moth reported by Liebhold [25]. During the early period of population growth (light or moderate level of infestation), the distribution of gypsy moth is more clumped compared to the peak of outbreaks. However, the opposite was true for *Holcocerus hippophaecolus* in heavily infested forests, where the larvae were distributed clumped. Random larval distribution was observed in forests with low populations [10]. This distribution pattern is mainly due to *H. hippophaecolus* adult females depositing eggs in large groups. *E. signifer* eggs are scattered individually. The young larvae live freely on the ground for a period of time before boring tree trunks causing damage [1]. Furthermore, *E. signifer* larvae are not aggregative. Therefore, when population density is high, the larvae disperse as random or uniform distributions and less clumped. Our site survey results reflected the same.

The large scale geostatistical analysis suggested that *E. signifer* larval spatial distribution was random when infestation level was light. The distribution was clumped when infestation level was moderate or severe. The spatial correlation was higher as the infestation level increased. Since *E. signifer* is a native species and naturally distributed in more than 50 counties of Guangxi, Eucalyptus trees are infested wherever planted in these areas. Therefore, lightly infested plantations were distributed across the entire province in a random manner. Heavily infested plantations were distributed in the central and southern areas of the province as the environmental conditions in these areas are favorable for Eucalyptus and *E. signifer*. The spatial distribution comparison between the small and large scales helps better understanding of insect population spatial structure and dynamics. Such knowledge can aid insect sampling and monitoring [10]. For example, Shi et al (1997) applied geostatistical method to produce density contour maps of overwinter pupae, egg mass and larvae of *Dendrolimus punctatus* Walker, which served as the bases for sampling, pest forecasting and management [19]. Furthermore, the current study also showed that *E. signifer* infestation was heavier in the 2nd generation forests than that the 1st generation forests. More attention should be paid to the 2nd generation forests regarding *E. signifer* monitoring and management.

E. signifer larvae rarely move from tree to tree once bored into tree trunks [1]. The spatial distribution pattern is

determined by host selection of the larvae. The factors influencing host selection is largely unknown. Analysis of survey results indicated that *E. signifer* larvae were clumped distributed at the tree trunks below 8 m. Above 8 m, the distribution pattern became random or uniform [2]. The larval distribution also tends to be clumped regardless of infestation level, forest type and age. But as infestation level and tree age increases, the distribution is less clumped. In addition, our surveys indicated that *E. signifer* preferred younger forests. For forests older than 4 years, mostly only one larva per tree was observed and distributed randomly. This distribution pattern probably is due to *E. signifer* switch host from native tree species to the introduced Eucalyptus and the mutually exclusive nature of the *E. signifer* larvae.

5. Conclusion

The *E. signifer* spatial distribution at plantation level (small scale) was clumped regardless of infestation level. At large scale level, the spatial distribution depends on its infestation. When the infestation was light, the distribution was random. When the infestation was moderate or severe, the distribution pattern was clumped. Additionally, the distribution of *E. signifer* larvae in the 2nd generation forests was more clumped and spatially depended than that in the 1st generation forests. These distribution patterns provide foundational knowledge of *E. signifer* infestation and damage of Eucalyptus forests, which would aid population forecast and damage evaluation.

References

- [1] Yang XH, Yu YH, Wu YJ, et al., First report of *Endoclyta signifer* (Lepidoptera: Hepialidae) as a new pest on Eucalyptus. *Journal of Economic Entomology*, 106:866-873 (2013).
- [2] Yang XH, Yu YH, Cao SG, et al., Morphology and biology of *Endoclyta signifer* Walker, a new borer damage on Eucalyptus. *Forest research*, 26: 34-40 (2013).
- [3] Qi SX, Eucalyptus in China. Beijing, Chinese Forest Press (2002).
- [4] Yang XH, Cheng SW, Yu YH, et al., Damage occurred monitoring and risk analysis of *Endoclyta signifer* Walker in Guangxi. *Anhui Agricultural Science Bulletin*., 18:84-86 (2012).
- [5] Qin JL, Yang XH, Fu H, and Lei XF, A novel nonlinear algorithm for area-wide near surface air temperature retrieval. *IEEE J. Sel. Top. Appl. Earth Obs. Remote Sens.*, 9:3283-3296 (2016).
- [6] Xu RM, Population ecology of insects. Beijing: Beijing Normal University Press (1987).
- [7] Ding YQ, Mathematical ecology of insects. Beijing, Science Press (1994).
- [8] Wang ZQ, Application of geostatistics in ecology. Beijing, Science Press (1999).

- [9] Wang ZJ, Li DM, Theories and methods of geostatistics and their application in insect ecology. *Entomological Knowledge*, 39:405-502 (2002).
- [10] Zong SX, Jia FY, Xu ZC, et al. Spatial distribution pattern and sampling method of *Holcocerus hippophaecolus* larvae. *Entomological Knowledge*, 41:552-555 (2004).
- [11] Zong SX, Luo YQ, Xu ZC, et al. Geostatistical analysis on spatial distribution of *Holcocerus hippophaecolus* eggs and larvae. *Acta Ecologica Sinica*, 25:831-836 (2005).
- [12] Zong SX. Studies on the bio-ecological characteristics of seabuckthorn carpenter moth: *Holcocerus hippophaecolus* (Lepidoptera:Cossidae). Doctoral dissertation, Beijing, Beijing Forestry University (2006).
- [13] Yuan ZM, Fu W, Li FY, Spatial distribution pattern of *Chilo suppressalis* analyzed by classical method and geostatistics. *Chinese Journal of Applied Ecology*, 15:610-614 (2004).
- [14] Williams L, Schotzko DJ, McCaffrey JP, Geostatistical description of the spatial distribution of *Limoniuss californicus* (Coleoptera: Elateridae) wire-worms in the northwestern United States, with comments on sampling. *Environ. Entomol.*, 21: 983-995 (1992).
- [15] Qin JL, Yang XH, Luo JT, et al. An improved novel nonlinear algorithm of area-wide near surface air temperature retrieval, *IEEE J. Sel. Top. Appl. Earth Obs. Remote Sens*, 11: 830-844 (2018).
- [16] Robertson GP, GS+ Geostatistics for the Environmental Sciences. Gamma Design Software, Plainwell, Michigan USA (2008).
- [17] Duarte F, Calvo MV, Borges A., and Scatoni IB, Geostatistics applied to the study of the spatial distribution of insects and its use in integrated pest management. *Rev. Agron. Noroeste Argent*, 35:9-20 (2015).
- [18] Southwood TRE, Henderson PA, Ecological Methods. 3rd ed. Blackwell Sciences, Oxford, 592 pp (2000).
- [19] Shi GS, Li DM, Geostatistic analysis of spatial pattern of *Dendrolimus punctatus*. *Chinese Journal of Applied Ecology*, 8:612-616 (1997).
- [20] Li HX, Guo SP, ZHou ZJ, et al. Spatial distribution pattern and sampling method of the larvae of *Phassus excrescens*. *Journal of Northwest Forestry University*, 24:140-142 (2009).
- [21] Schotzko DJ and O'Keefe LE, Geostatistical description of the spatial distribution of *Lygus hesperus* (Heteroptera: Miridae) in lentils. *J. Econ. Entomol.*, 82:1277-1288 (1989).
- [22] Cao SG, Pang ZH, Yang XH, et al. Preliminary study on spatial distribution pattern of *Endoclyta signifer* Walker Larva. *Journal of Anhui Agri. Sci.*, 39:11492-11495 (2011).
- [23] Midgarden DG, Youngman RR, Fleischer SJ, Spatial analysis of counts of western corn root worm (Coleoptera: Chrysomelidae) adults on yellow sticky traps in corn: geostatistics and dispersion indices. *Environ. Entomol.*, 22: 1124-1133 (1993).
- [24] Li YC, Xia NB, Tu UQ, et al. A geostatistical analysis on spatial patterns of *Anoplophora glabripennis* in poplars. *Acta Ecologica Sinica*, 17:301-309 (1997).
- [25] Liebhold AM, Rossi RE, Kemp WP, Geostatistics and geographic information systems in applied insect ecology. *Annu. Rev. Entomol.*, 38: 303-327 (1993).